



## On the miscibility of cardiolipin with 1,2-diacyl phosphoglycerides: Binary mixtures of dimyristoylphosphatidylethanolamine and tetramyristoylcardiolipin <sup>☆</sup>

Maria Frias <sup>a</sup>, Matthew G.K. Benesch <sup>b</sup>, Ruthven N.A.H. Lewis <sup>b</sup>, Ronald N. McElhaney <sup>b,\*</sup>

<sup>a</sup> Faculty of Pharmacy and Biochemistry, University of Buenos Aires, Buenos Aires, Argentina

<sup>b</sup> Department of Biochemistry, School of Molecular and Systems Medicine, Faculty of Medicine and Dentistry, University of Alberta, Edmonton, Alberta, Canada T6G 2H7

### ARTICLE INFO

#### Article history:

Received 26 May 2010

Received in revised form 5 December 2010

Accepted 11 December 2010

Available online 21 December 2010

#### Keywords:

Cardiolipin

Phosphatidylethanolamine

Thermotropic phase behavior

Lipid bilayer

Differential scanning calorimetry

Infrared spectroscopy

### ABSTRACT

The thermotropic phase behavior and organization of model membranes composed of binary mixtures of the quadruple-chained, anionic phospholipid tetramyristoylcardiolipin (TMCL) with the double-chained zwitterionic phospholipid dimyristoylphosphatidylethanolamine (DMPE) were examined by a combination of differential scanning calorimetry (DSC) and Fourier-transform infrared (FTIR) spectroscopy. After equilibration at low temperature, DSC thermograms exhibited by binary mixtures of TMCL and DMPE containing <80 mol DMPE exhibit a fairly energetic lower temperature endotherm and a highly energetic higher temperature endotherm. As the relative amount of TMCL in the mixture decreases, the temperature, enthalpy and cooperativity of the lower temperature endotherm also decreases and is not calorimetrically detectable when the TMCL content falls below 20 mol%. In contrast, the temperature of the higher temperature endotherm increases as the proportion of TMCL decreases, but the enthalpy and cooperativity both decrease and the transition endotherms become multimodal. The FTIR spectroscopic results indicate that the lower temperature endotherm corresponds to a lamellar crystalline ( $L_c$ ) to lamellar gel ( $L_\beta$ ) phase transition and that the higher temperature transition involves the conversion of the  $L_\beta$  phase to the lamellar liquid-crystalline ( $L_\alpha$ ) phase. Moreover, the FTIR spectroscopic signatures observed at temperatures below the onset of the  $L_c/L_\beta$  phase transitions are consistent with the coexistence of structures akin to a TMCL-like  $L_c$  phase and the  $L_\beta$  phase, and with the relative amount of the TMCL-like  $L_c$  phase increasing progressively as the TMCL content of the mixture increases. These latter observations suggest that the TMCL and DMPE components of these mixtures are poorly miscible at temperatures below the  $L_\beta/L_\alpha$  phase transition temperature. Poor miscibility of these two components is also suggested by the complexity of the DSC thermograms observed at the  $L_\beta/L_\alpha$  phase transitions of these mixtures and with the complex relationship between their  $L_\beta/L_\alpha$  phase transition temperatures and the composition of the mixture. Overall, our data suggests that TMCL and DMPE may be intrinsically poorly miscible across a broad composition range, notwithstanding the homogeneity of the fatty acid chains of the two components and the modest ( $\sim 10^\circ\text{C}$ ) difference between their  $L_\beta/L_\alpha$  phase transition temperatures.

© 2010 Elsevier B.V. All rights reserved.

**Abbreviations:** DMPE, dimyristoylphosphatidylethanolamine; CL, cardiolipin; PE, phosphatidylethanolamine; DMPG, dimyristoylphosphatidylglycerol; DMPC, dimyristoylphosphatidylcholine; TMCL, 1,2-,1',2'-tetramyristoylcardiolipin; DSC, differential scanning calorimetry; IR, infrared; FTIR, Fourier-transform infrared; C=O, carbonyl; CH<sub>2</sub>, methylene;  $L_\alpha$ , lamellar liquid-crystalline;  $L_\beta$ , lamellar gel;  $L_c$ , lamellar crystalline;  $T_m$ , gel/liquid-crystalline phase transition temperature

<sup>☆</sup> Supported by operating and major equipment grants from the Canadian Institutes of Health Research (RNM), major equipment grants from the Alberta Heritage Foundation for Medical Research (RNM), a travel support grant from the Consejo Nacional de Investigaciones Científicas y Técnicas (MF), and summer studentships from the Natural Sciences and Engineering Research Council of Canada and the Alberta Heritage Foundation for Medical Research (MGKB).

\* Corresponding author. Tel.: +1 780 492 2413; fax: +1 780 492 0886.

E-mail address: [rmcelhan@ualberta.ca](mailto:rmcelhan@ualberta.ca) (R.N. McElhaney).

### 1. Introduction

The structure and organization of lipid bilayer model membranes derived from mixtures of two or more lipids are of special biological importance because the lipid components of all cell membranes are heterogeneous mixtures of different classes and molecular species of lipids. This fact has provided the impetus for numerous studies of the thermotropic phase behavior and mixing properties of a wide range of lipid mixtures [see 1]. The results of such studies are usually expressed as temperature-composition pseudo phase diagrams, from which important information about the miscibility of specific lipid components can be obtained. The importance of such studies has now come into sharper focus because of suggestions that cell membranes may contain laterally segregated, compositionally distinct domains that may be essential for the normal functioning of membrane proteins and transmembrane signaling systems [see 2–6].

Of the limited number of studies of mixtures of different classes of phospholipids that have been performed, relatively few have been on cardiolipin (CL<sup>1</sup>)-containing systems, presumably because this anionic, quadruple-chained lipid is not a major component of most mammalian cell membranes. However, CL is an important component of the plasma membranes of many types of Gram-negative and Gram-positive bacteria, and of the mitochondrial and chloroplast inner membranes of eukaryotes [7–11]. CL is usually a relatively small component ( $\leq 10$  mol%) of such membranes, where its primary role appears to be that of supporting the function of key membrane proteins [7]. The consensus of currently available data is that CL is important for the structural stabilization and activation of many mitochondrial enzymes, especially those involved in ATP synthesis and energy transduction [12–18], and for maintaining the structure and function of the Type II photoreaction center of photosynthetic bacteria and plants [19]. In higher eukaryotes, CL is an effector of the cytochrome P-450-dependent cholesterol side-chain cleavage enzyme and activates cytochrome c oxidase and the mitochondrial phosphate carrier protein [20–22]. In fact, it has been suggested that the capacity for structurally specific interactions with membrane CL may actually be highly conserved in such proteins [23]. CL may also be found in substantially higher quantities (~55–60 mol%) in the membranes of some microbial organisms, wherein elevated levels of CL and its derivatives appear to enhance the tolerance of these organisms to halophilic and resource-depletion stress [11,24–26]. The study of CL-containing membranes is thus an important aspect of the understanding of the membrane properties required to support the function of many of cellular mechanisms, including those involved in energy procurement and transduction [26,27].

Relatively few studies of CL membranes, and of membranes composed of mixtures of CL with other lipids, have been performed. In part, this is because the chemical synthesis of stereochemically pure CL has not been as straight forward as with most other naturally occurring phospholipids, so that only a few species of stereochemically pure, synthetic CL are currently commercially available. Thus, most of the studies of CL-containing membranes have been performed with mixtures composed of highly unsaturated CLs isolated from natural sources (predominantly beef heart) and various other types of naturally occurring and synthetic phospholipids, and the general consensus of such studies have been that CL is highly immiscible with most other lipids [see 28 and references cited therein]. However, an unambiguous interpretation of many of these results is often difficult, because there are considerable differences between the length and degree of unsaturation of the hydrocarbon chains of the CL and non-CL components of the mixture. It is therefore difficult to disentangle the potential effects of variations in the polar headgroup composition of the mixture from the known effect of variations in fatty acyl group length and degree of unsaturation on phospholipid miscibility [see 28 and references cited therein]. To circumvent such problems, we are studying the interactions of stereochemically pure, synthetic TMCL with various dimyristoyl glycerophospholipids. We present here the results of a detailed study of binary mixtures of di-anionic TMCL with zwitterionic DMPE using a combination of high-sensitivity DSC and FTIR spectroscopy. This study encompasses all aspects of the polymorphic phase behavior exhibited by these mixtures and addresses a number of fundamental issues related to the overall miscibility of these two lipids and the general principles underlying lipid/lipid interactions in all of the polymorphic phases formed. PE is a major component of many eukaryotic membranes, and PE and CL are both found in many prokaryotic surface membranes and in the mitochondrial inner membranes of most eukaryotic cells. The study of the structure and organization of PE/CL model membranes and of the miscibility of these lipids is thus biologically relevant.

## 2. Materials and methods

The phospholipids TMCL and DMPE were obtained from Avanti Polar Lipids Inc. (Alabaster, AL) and used without further purification. Binary mixtures were prepared by mixing chloroform:methanol (9:1) solutions of the lipids in the amounts required to obtain the desired composition. The solvent was then slowly removed in a stream of nitrogen such that the lipid mixture was cast as a thin film on the sides of a clean glass tube whilst maintaining a temperature near 60 °C. The lipid film was then dried *in vacuo* overnight to ensure removal of the last traces of solvent. Hydration of the lipid film was achieved by placing some wet cotton wool into the tube (without contacting the lipid film) and allowing the sample to absorb water from the water vapor-saturated air by warming the sample to temperatures near 60 °C. Subsequently, the cotton wool was removed and the hydrated sample was quickly dispersed in pre-warmed buffer composed of 100 mM phosphate, 5 mM Na<sub>2</sub>N<sub>3</sub>, 150 mM NaCl, pH 7.4 and mixed by vigorous vortex mixing at temperatures near 60 °C. In one set of measurements, samples containing 3–4  $\mu$ mol of lipid were dispersed in 600  $\mu$ l of buffer and a 500  $\mu$ l aliquot was introduced into the hastelloy capsule of a Calorimetry Sciences Corporation (Spanish Fork, UT) high-sensitivity, heat-conduction Multi-Cell DSC instrument. Prior to initial data acquisition, the sample was preconditioned by heating to 60 °C followed by cooling to –7 °C at scanning rates near 60 °C/h. Data acquisition scans were then performed at scanning rates near 10 °C/h. Typically, the process first involves three cycles of heating and cooling between –7 °C and 60 °C. Subsequently, the samples were cooled to –30 °C and incubated at that temperature 12 h, then heated to 5 °C and incubated at that temperature to ensure that all ice had completely melted. This low temperature incubation protocol was repeated twice and the sample was then cooled to –7 °C and a further set of data acquisition runs, consisting of two cycles of heating and cooling between –7 °C and 60 °C, were performed. In a companion set of DSC measurements, samples containing ~1 mg of lipid were dispersed in 1 ml of buffer by methods similar to those described above. Subsequently, 323  $\mu$ l aliquots were loaded into a high-sensitivity power-compensation nano-DSC instrument (Calorimetry Sciences Corporation) and data were acquired between 0 and 60 °C at heating and cooling rates near 10 °C/h. The measurements performed in the Multi-Cell DSC enabled an accurate mapping of the gel phase polymorphic behavior of these samples, whereas those in the Nano-DSC measurements enabled more accurate mapping of the boundaries of the gel/liquid-crystalline phase transitions of the various lipid mixtures examined. The data acquired were analyzed and plotted with the Origin software package (OriginLab Corporation, Northampton, MA).

FTIR spectroscopy was performed on samples containing 2–4 mg of lipid. Samples were dispersed as described above in 50–75  $\mu$ l of a D<sub>2</sub>O-based buffer containing 100 mM phosphate, 150 mM NaCl, pH 7.4. The dispersion was squeezed between the CaF<sub>2</sub> windows of a heatable, demountable liquid cell (NSG Precision Cells, Farmingdale, NY) equipped with a 25  $\mu$ m Teflon spacer. Once mounted in the sample holder of the spectrometer, the sample could be heated between –20 °C and 90 °C by an external, computer-controlled water bath. Prior to initial data acquisition, samples were subject to the same low temperature incubation protocol described above for the DSC samples. Infrared spectra were then acquired as a function of temperature with a Digilab FTS-40 Fourier-transform Spectrometer (Biorad, Digilab Division, Cambridge, MA) using data acquisition parameters similar to those described by Mantsch et al. [29]. The experiment involved a sequential series of 2 °C temperature ramps with a 20-minute inter-ramp delay for thermal equilibration, and was equivalent to an effective scanning rate of 4 °C/h. The data obtained were analyzed using computer programs obtained from the instrument manufacturer and from the National Research Council of Canada. In cases where absorption bands appeared to be a summation

<sup>1</sup> See Abbreviations.

of components, a combination of Fourier deconvolution and curve-fitting procedures were used to obtain estimates of the position of the component bands and to reconstruct the contours of the original band envelope.

### 3. Results

#### 3.1. Differential scanning calorimetric studies

Heating and cooling DSC thermograms which exemplify the thermotropic phase behavior exhibited by aqueous dispersions of pure DMPE and pure TMCL are presented in Fig. 1. The details of the thermotropic phase behavior of these two phospholipids individually have been described fully elsewhere [see 30,31 and references cited therein], but are briefly summarized to allow direct comparison with the behavior of the binary mixtures. As illustrated in Fig. 1A, freshly prepared aqueous dispersions of pure DMPE exhibit a highly cooperative and highly energetic ( $\Delta H_{\text{cal}} \sim 6$  kcal/mol) endothermic peak centered near 50 °C upon heating. A combination of spectroscopic and other physical techniques have shown that this process is essentially a hydrocarbon chain-melting phase transition from a lamellar gel ( $L_{\beta}$ ) to a lamellar liquid-crystalline ( $L_{\alpha}$ ) phase [see 30, and references cited therein]. Upon cooling, the  $L_{\alpha}$  phase of DMPE reconverts to the  $L_{\beta}$  phase at temperatures near 50 °C. However, this process is usually associated with two exothermic peaks, the occurrence of which has been assigned to domain heterogeneity in the  $L_{\alpha}$  phase [30,32]. Fig. 1A also shows that after extensive equilibration at low temperatures, the  $L_{\beta}/L_{\alpha}$  phase transition near 50 °C is suppressed and replaced by a considerably more energetic phase transition ( $\Delta H_{\text{cal}} \sim 18$  kcal/mol) at temperatures near 58 °C. The latter transition has been assigned to the direct conversion of the lamellar crystalline ( $L_c$ ) form of the lipid to the  $L_{\alpha}$  phase [see 30 and references cited therein]. In contrast, the DSC thermograms exhibited by freshly prepared samples of TMCL typically contain relatively broad, moderately energetic endotherms at temperatures between 10 and 20 °C and between 25 and 30 °C, and a higher temperature endotherm centered near 40 °C (see Fig. 1B). The two lower temperature events both arise from the conversion of  $L_c$  domains of TMCL to the  $L_{\beta}$  phase and the high temperature event near 40 °C represents the conversion of the  $L_{\beta}$  phase to the  $L_{\alpha}$  phase [31]. Upon cooling, the higher temperature event is shown to be fully reversible and a single the lower temperature endotherm is typically observed at

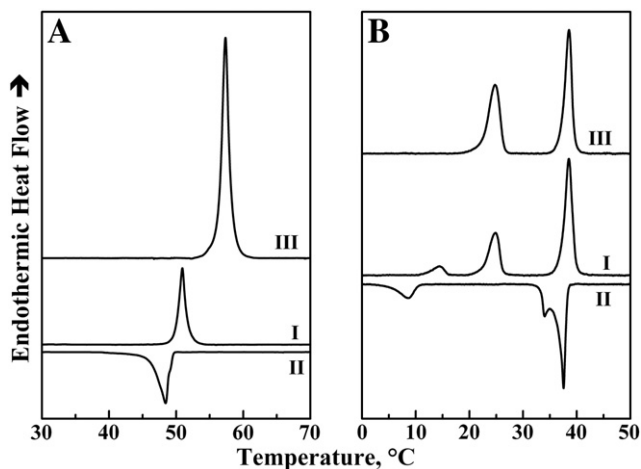


Fig. 1. DSC thermograms illustrating the polymorphic phase behavior exhibited by aqueous dispersions of pure DMPE (A), and pure TMCL (B). In each panel the thermograms labeled I and II, respectively, illustrate the heating and cooling behavior exhibited by freshly prepared samples, and the thermograms labeled III illustrate the heating behavior initially observed after increasing periods of incubation at low temperatures. The thermograms shown were acquired at scanning rates near 10 °C/h.

temperatures near 8 °C. Fig. 1B also shows that after extensive low temperature incubation, the weak endotherm between 10 and 20 °C is completely suppressed and that the intensity of the endotherm centered between 25 °C and 30 °C increases significantly, while the properties of the higher temperature endotherm near 40 °C are unaffected. This behavior has been ascribed to the annealing of small domains of  $L_c$  TMCL into larger domains that are structurally similar [31]. For such samples, the enthalpies of the lower- and higher temperature transitions are  $\sim 11.9$  kcal/mol and  $\sim 12.9$  kcal/mol, respectively [31].

The stacked plots shown in Fig. 2 illustrate the pattern of DSC thermograms which typify the thermotropic phase behavior of model membranes composed of binary mixtures of DMPE and TMCL (mol fraction range 0.05–0.95) observed upon initial heating after prolonged incubation at low temperature (Fig. 2A) and upon cooling (Fig. 2B). With the probable exception of those mixtures of high (>80 mol%) DMPE content, the heating thermograms observed after low temperature sample equilibration contain a lower temperature transition centered at temperatures between 15 °C and 30 °C, a process assigned to the solid-phase transition between  $L_c$  and  $L_{\beta}$  domains (see FTIR spectroscopic studies). As illustrated in Fig. 2B, this event exhibits considerable hysteresis ( $\sim 10$  °C–20 °C) upon cooling, and with the probable exception of those mixtures containing at least 70 mol% TMCL, the reversal process is not usually resolved in cooling exotherms. Fig. 2 also shows that all mixtures exhibit a highly energetic, higher temperature heating endotherm at temperatures between 40 °C and 50 °C (Fig. 2A) which is not affected by the low temperature incubation protocols used. This transition involves the cooperative melting of the lipid hydrocarbon chains such as occurs when the  $L_{\beta}$  phase converts to the  $L_{\alpha}$  phase (see FTIR spectroscopic results) and, as illustrated in Fig. 2B, the reversal of the process occurs over a comparable temperature range upon cooling, albeit with a slight hysteresis.

Fig. 2 also shows that the characteristics of each of these transitions vary significantly with the composition of the binary DMPE:TMCL mixtures and that the composition-dependent changes in the properties of these two thermotropic events are markedly different. The endothermic peaks arising from  $L_c/L_{\beta}$  phase transitions observed upon heating well equilibrated samples of these DMPE–

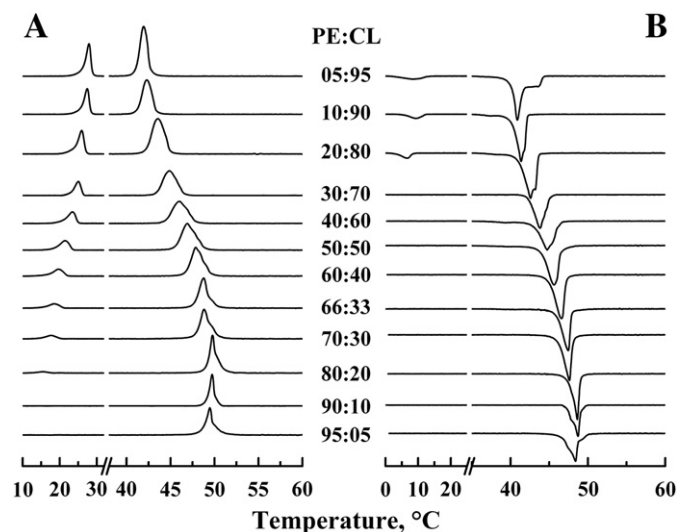


Fig. 2. DSC thermograms illustrating the composition-dependent changes exhibited by model membranes composed of binary mixtures of DMPE and TMCL. Panel A (left) shows the heating endotherms which typify the behavior observed upon initial heating of the samples after prolonged annealing at low temperature and panel B (right) shows the exothermic events observed upon cooling. The data shown were acquired at the DMPE:TMCL ratios as indicated and were recorded with the Multi-Cell DSC instrument operating at scan rates near 10 °C/h.

TMCL mixtures are generally asymmetric in shape with significant low temperature tailing. We find that the widths of these peaks tend to increase as the TMCL content of the mixture increases, but the overall asymmetry in shape is largely maintained at all compositions at which these peaks are resolved. These peaks are typically centered between 15 and 30 °C and their midpoint temperatures decrease progressively as the TMCL content of the mixture decreases. However, the areas under these peaks decrease progressively as the TMCL content of the mixture decreases, to the extent that discrete  $L_c/L_\beta$  phase transitions are not calorimetrically detectable when the mol fraction of TMCL falls below 20 mol%. In contrast, peaks defining the  $L_\beta/L_\alpha$  phase transitions of these mixtures are observed at all lipid compositions and their mid-point transition temperatures and transition enthalpies fall within the range defined by the transition temperatures and transition enthalpies of the pure lipid components. However, the shapes of these peaks seem to be defined by a very complex function of lipid composition, and for many of these mixtures the observed peaks seem to be a composite of two or more components. This complex pattern of behavior is probably indicative of marked changes in the interactions between and/or the miscibility of these two components at temperature near to the  $L_\beta/L_\alpha$  phase transitions of the mixtures.

The effects of composition on the mid-point temperatures and enthalpies of the calorimetrically resolved phase transitions exhibited by the binary DMPE:TMCL mixtures are summarized in the graphs shown in Fig. 3. In the composition range examined (0.05–0.95 mol fraction DMPE), the temperatures and enthalpies of the  $L_\beta/L_\alpha$  phase transitions of the mixtures both describe curvilinear functions of the lipid composition, with the curvature approaching maximal values in the DMPE-rich regions of the phase diagram. The nonlinearity of the thermodynamic parameters of the  $L_\beta/L_\alpha$  phase transitions of these mixtures as a function of the lipid composition is generally consistent with the non-ideal mixing of the components at temperatures at or near to their  $L_\beta/L_\alpha$  phase transition temperatures [1]. With the  $L_c/L_\beta$

phase transitions of these mixtures, discrete thermotropic transitions were only discernable over the compositional range 0.05–0.8 mol fraction DMPE (see Fig. 3), and the midpoint temperatures and transition enthalpy values of these transitions both described a near linear function of lipid composition (see Fig. 3), with the enthalpy values effectively vanishing when the DMPE content of the mixture exceeds 80 mol%. The effective disappearance of the  $L_c/L_\beta$  phase transitions from the DMPE-rich ( $\geq 80$  mol%) mixtures, along with the fact that the general characteristics of the transition endotherms exhibited by the TMCL-rich mixtures seem to approach those exhibited by pure TMCL, suggests that the appearance of these transitions may actually be TMCL-driven. As will be demonstrated later, this suggestion is strongly supported by our FTIR spectroscopic data.

As noted above, CL is a quadruple-chained amphiphile and as a result, mixtures of CL with the common double-chained phospholipids will contain disproportionately larger fractions of cardiolipin-derived fatty acyl chains. We have therefore examined the variation of the transition temperatures and transition enthalpy values of the two transitions as a function of the mol fraction of TMCL chains in the mixture and the results are summarized in Fig. 3. These results show that the temperatures of the  $L_\beta/L_\alpha$  phase transitions of these mixtures are not correlated with the mol fraction of TMCL chains in the mixture, and that there is also a poor correlation between these transition temperatures and the mol fraction of DMPE chains in the mixtures (Fig. 3, Panel A). However, there does appear to be an excellent correlation between the enthalpy of the  $L_\beta/L_\alpha$  phase transitions and the mol fraction of TMCL chains in the mixture (Fig. 3, Panel B). However, the reverse seems to be the case with the  $L_c/L_\beta$  phase transitions, for which there seems to be a good correlation between the transition temperatures and the mol fraction of TMCL chains, but a poor correlation between the enthalpy values measured and the mol fraction of TMCL chains (Fig. 3, Panels C and D). Undoubtedly, the differences between these aspects of the behavior of the two phase

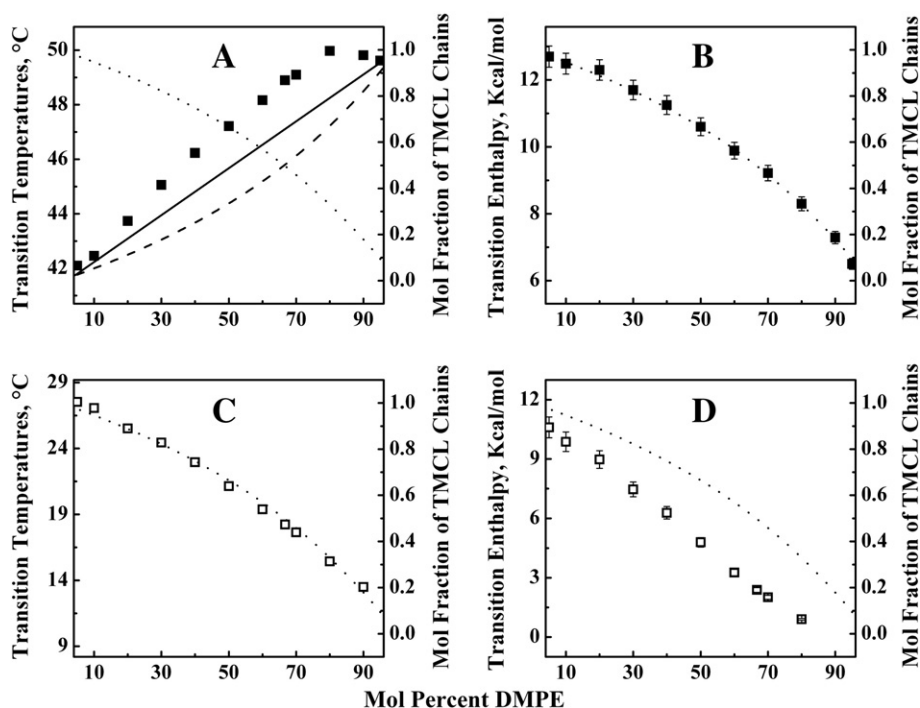


**Fig. 3.** Effect of lipid composition on the transition temperature and transition enthalpy changes of the  $L_\beta/L_\alpha$  (■) and  $L_c/L_\beta$  (□) phase transitions exhibited by binary mixtures of DMPE and TMCL. The mid-point temperatures reported were the temperatures of 50% conversion as estimated from the area integrals. In each panel, the data points are the experimentally determined values ( $\pm$  measurement error) overlaid on the curve (dotted line) illustrating the changes in the mol fraction of TMCL hydrocarbon chains as a function of lipid composition. In panel A, the dashed line illustrates the curve describing the changes in the mol fraction of DMPE hydrocarbon chains as a function of the DMPE content of the mixture and the solid line describes the composition-dependent changes in the  $L_\beta/L_\alpha$  phase transition temperature expected of a system of binary mixtures in which there is ideal mixing of the two components.

transitions reflects fundamental differences in the structural phenomena underlying the two types of phase transitions and in way in which they are affected by changes in the composition of the lipid mixture (see Discussion).

### 3.2. Fourier transform infrared spectroscopic studies

Illustrated in Fig. 4 are the C=O stretching and CH<sub>2</sub> scissoring bands exhibited by the three lamellar phases formed by pure samples of DMPE and TMCL. Detailed descriptions and structural interpretations of the spectroscopic data shown therein have been presented elsewhere [30,31], but are briefly summarized here as references against which the behavior of the binary mixtures can be compared. In the L<sub>α</sub> phase (spectra III), both lipids exhibit relatively broad absorption bands, consistent with the high mobility of the vibrating groups examined. These absorption bands sharpen significantly when samples are cooled to gel phase temperatures (see spectra II), consistent with the overall decrease in the mobility of all vibrating groups which occurs at the transition from the L<sub>α</sub> to the L<sub>β</sub> phase. Fig. 4 also shows that the CH<sub>2</sub> scissoring and C=O stretching bands of DMPE and TMCL sharpen even further upon annealing to their respective L<sub>c</sub> phases, such that distinctive patterns of infrared absorption can be discerned (spectra I). These latter spectroscopic features are the result of further immobilization of the various vibration groups to an extent that enables specific patterns of close-contact interactions between hydrocarbon chains in the bilayer core and of distinct patterns of hydration and hydrogen-bonding interactions in the polar/apolar interfacial regions of the two phospholipid bilayers [for details, see Refs. 30,31]. However, the differences between the spectroscopic signatures of the L<sub>c</sub>, L<sub>β</sub>, and L<sub>α</sub> phases of each lipid are quite distinct, thus facilitating the detection of transitions between the various phases of these lipids. Moreover, from a comparison of the spectroscopic signatures of the various phases of DMPE with those of comparable phases of TMCL, it is apparent that the spectroscopic characteristics of the L<sub>β</sub> and L<sub>α</sub> phases of the two lipids are generally similar (though not identical, see Refs. [30,31]), whereas those of the L<sub>c</sub> phases of the two lipids are markedly different. This latter property aided the assignment of the nature of the phase transitions exhibited by the various binary mixtures and

development of a structural interpretation of their spectroscopic characteristics.

The stacked plots shown in Figs. 5 and 6 exemplify the pattern of thermally induced spectroscopic changes exhibited by the mixed DMPE:TMCL model membranes examined. In both heating and cooling measurements, the spectroscopic data show evidence of thermally-induced discontinuities at temperatures comparable to the range spanned by the phase transitions resolved by DSC. Upon heating samples that have been equilibrated at low temperature, the C=O stretching and CH<sub>2</sub> scissoring regions of the IR spectra both show low and high temperature discontinuities (Fig. 5, panels A and B), whereas the C–H stretching region shows evidence of a single discontinuity (Fig. 5, panel C) occurring at temperatures comparable to that spanned by the high temperature discontinuities observed in the C=O stretching and CH<sub>2</sub> scissoring regions. With most of the mixtures examined, the FTIR spectroscopic data observed upon cooling show a single discontinuity at temperatures comparable to those of the higher temperature discontinuity observed upon heating (Fig. 6). However, with some of the TMCL-rich samples, there is also evidence for an additional discontinuity at temperatures some ~10 °C lower than the range spanned by the lower temperature transition observed upon cooling (data not shown).

The single higher temperature discontinuity observed in the C–H stretching region of the FTIR spectroscopic data observed upon heating and cooling is manifest by a discontinuous 2–5 cm<sup>-1</sup> increase/decrease in the frequencies of the symmetric and asymmetric CH<sub>2</sub> stretching bands centered near 2850 cm<sup>-1</sup> and 2920 cm<sup>-1</sup>, respectively, and by an overall broadening of those bands (see Fig. 5, panel C). This combination of characteristics is consistent with the increase/decrease in hydrocarbon chain conformational order and with the increase/decrease in overall molecular mobility which occurs upon melting/freezing of the lipid hydrocarbon chains [33,34]. The higher temperature events resolved upon heating these mixtures are thus hydrocarbon chain-melting phase transitions which, as shown here by both DSC (Fig. 2) and FTIR spectroscopy (Fig. 6), are fully reversible upon cooling over comparable temperature ranges. Higher temperature discontinuities coincident with the cooperative melting/freezing of the hydrocarbon chains are also observed in the CH<sub>2</sub> scissoring and C=O stretching region of the IR spectrum (Figs. 5 and 6). In the CH<sub>2</sub> scissoring region, the process is manifest upon heating primarily by discontinuous increases in the linewidth and decreases in the intensity of the main CH<sub>2</sub> scissoring band near 1468 cm<sup>-1</sup> without significant changes in the peak frequency. These changes are consistent with the increases in methylene group mobility and decreases in the strength of the lateral interactions between such groups which occur when lipid hydrocarbon chains melt [33,34], and are fully reversible upon cooling over a comparable temperature range. In the C=O stretching region of the IR spectrum, the high temperature discontinuities which occur at the L<sub>β</sub>/L<sub>α</sub> phase transition are manifest primarily by changes in the component structure of the absorption band. In the L<sub>β</sub> and L<sub>α</sub> phases of most 1,2-diacyl glycerolipids, the C=O absorption bands are usually summations of components centered near 1743 cm<sup>-1</sup> and 1728 cm<sup>-1</sup>, which arise from the stretching vibrations of populations of free and H-bonded ester carbonyl groups, respectively [33,34]. The transitions between the L<sub>β</sub> and L<sub>α</sub> phases of most common phospholipids and the binary mixtures examined here are manifest primarily by reversible changes in the relative sizes of these populations (for an example, see Fig. 7).

The lower temperature discontinuities in the temperature-dependent changes in the FTIR spectra of these lipid mixtures occur predominantly in the CH<sub>2</sub> scissoring and C=O stretching bands. Moreover, such phenomena are normally observed at temperatures below the onset of the L<sub>β</sub>/L<sub>α</sub> phase transition upon initial heating, after prolonged low temperature equilibration of samples which contain at least 20 mol% TMCL [Figs. 5 and 6]. At low temperatures, the dominant features observed in the CH<sub>2</sub> scissoring region of the FTIR spectra of such samples are the main CH<sub>2</sub> scissoring

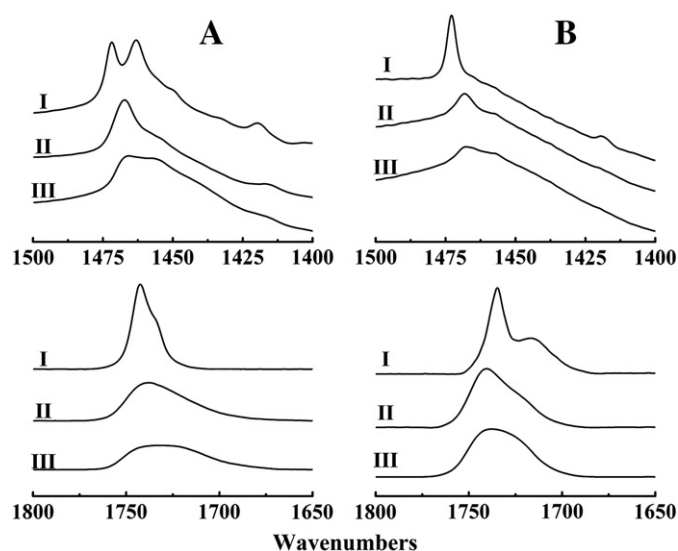


**Fig. 4.** The CH<sub>2</sub> scissoring (top) and C=O stretching (bottom) regions of the infrared spectra exhibited by the polymorphic phases formed by aqueous dispersions of DMPE (Panel A) and TMCL (panel B). Absorbance spectra are presented for: I. The lamellar crystalline (L<sub>c</sub>) phase. II. The lamellar gel (L<sub>β</sub>) phase. III. The lamellar liquid-crystalline (L<sub>α</sub>) phase.

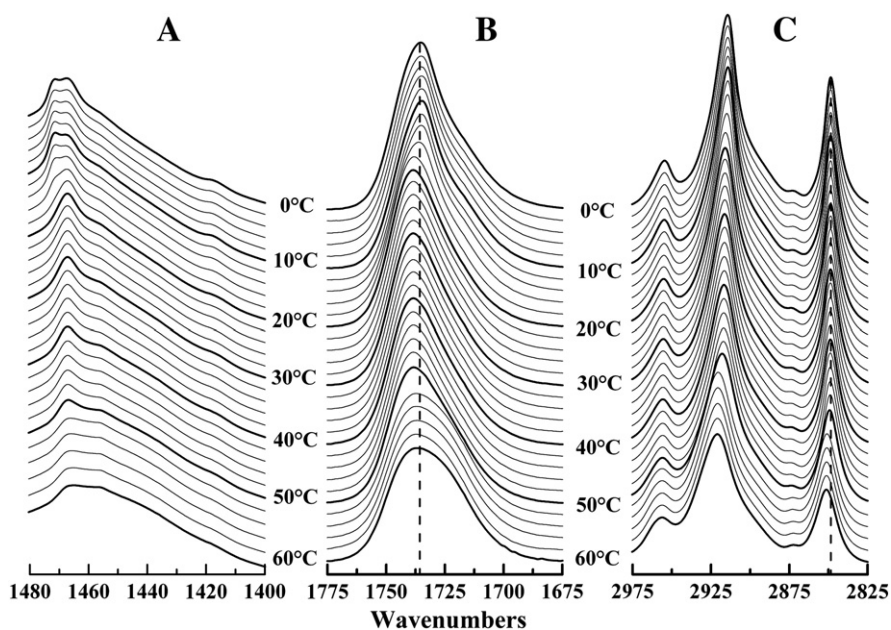


**Fig. 5.** Stacked plot illustrating the temperature-dependent changes in the CH<sub>2</sub> scissoring (A), C=O stretching (B) and C–H stretching bands (C) exhibited by model membranes derived from a binary 80:20 (mol:mol) mixture of DMPE and TMCL. The absorbance spectra presented were acquired upon heating after prolonged incubation at low temperature.

bands, which appear to be composed of two components centered near 1468 cm<sup>-1</sup> and 1472 cm<sup>-1</sup> (see Fig. 5). Upon heating through the calorimetrically resolved range of the lower temperature phase transition, the higher frequency component near 1472 cm<sup>-1</sup> progressively decreases in intensity, and disappears completely when the transition is complete. With hydrocarbon chain-containing compounds such those studied here, such changes in the contours of the CH<sub>2</sub> scissoring band are largely the result of changes in the lateral packing interactions between all-*trans* hydrocarbon chains [33,34]. These spectroscopic changes in the CH<sub>2</sub> scissoring region are thus indicative of solid-state reorganization of the lipid hydrocarbon chains, such as occurs when the L<sub>c</sub> phase of a lipid converts to the L<sub>β</sub> phase [33,34].

In the C=O stretching region of the IR spectra exhibited by these lipids, the dominant feature is the broad absorption band envelope centered near 1735 cm<sup>-1</sup>, which arises from the stretching vibrations of the ester carbonyl groups located at the polar/apolar interfacial regions of these lipid bilayers [33,34]. At temperatures below the onset of the lower temperature transition resolved by DSC, well equilibrated samples of mixtures which contain at least 10 mol% TMCL exhibit a complex band contour which seems to be composed of components centered near 1743, 1734, 1725 and 1713 cm<sup>-1</sup> (see Fig. 7). Upon heating through the calorimetrically resolved range of the lower temperature phase transition, a major reorganization of the component structure occurs, such that at upon completion of the

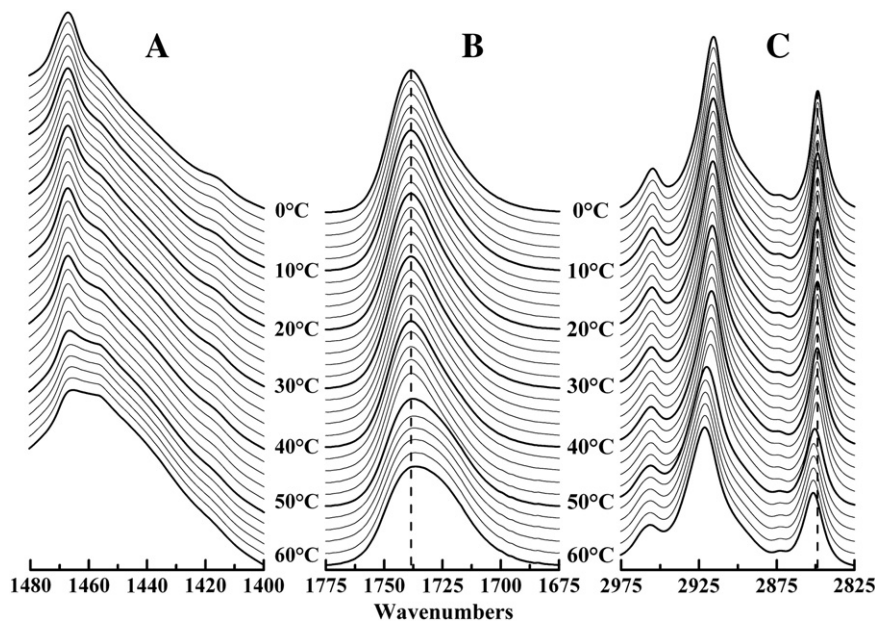


**Fig. 6.** Stacked plot illustrating the temperature-dependent changes in the CH<sub>2</sub> scissoring (A), C=O stretching (B) and C–H stretching bands (C) exhibited by model membranes derived from a binary 80:20 (mol:mol) mixture of DMPE and TMCL. Data are presented as the absorbance spectra observed upon cooling a sample from temperatures above the gel/liquid-crystalline phase transition.

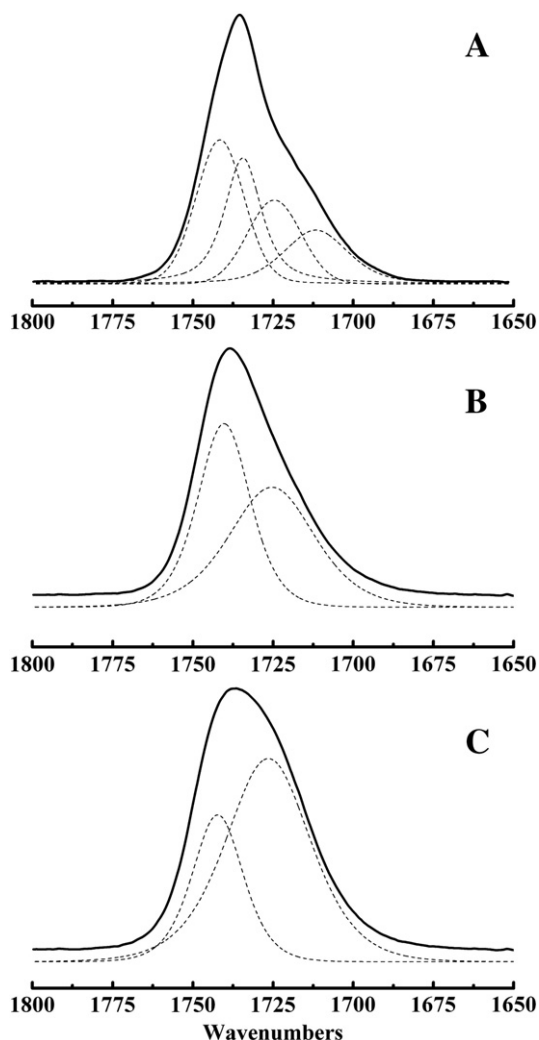


**Fig. 7.** Component structure of the C=O stretching bands exhibited by the lamellar phases formed by binary mixtures of TMCL and DMPE. The data shown were obtained from component analyses of the  $L_c$  (A),  $L_\beta$  (B) and  $L_\alpha$  (C) phases formed by an equimolar mixture of DMPE and TMCL, and typify our observations of all TMCL:DMPE mixtures in the composition range 5–95 mol% DMPE. Data are presented as absorbance spectra with the solid lines representing the observed C=O bands and the dashed lines our estimates of the absorption bands of the sub-populations. The latter are offset from the baseline for clarity.

phase transition, the four components alluded to above are replaced by the two components near  $1743\text{ cm}^{-1}$  and  $1728\text{ cm}^{-1}$ , components which typify the  $L_\beta$ -type gel phases formed by these lipid mixtures (see Fig. 7). With hydrated lipid bilayers, changes in the component structure of the ester carbonyl bands are usually attributed to changes in the hydration and/or the hydrogen-bonding interactions to the interfacially located ester carbonyl groups [33,34]. Given this and the fact that such changes occur at temperatures well below the onset of the hydrocarbon chain-melting phase transition, we conclude that the underlying process is a solid-state reorganization of hydration and hydrogen-bonding interactions at the bilayer polar/apolar interface, such as occurs when the  $L_c$  phase of a lipid converts to the  $L_\beta$  phase [33,34]. We also note that although discrete lower temperature phase transitions were not resolved in the DSC thermograms exhibited by mixtures containing less than 20 mol prevent TMCL (Fig. 2), spectral subtraction analyses of our FTIR spectroscopic provide evidence for the formation of the  $L_c$  phase in mixtures containing ~10 mol% TMCL (see below), suggesting that the putative phase transition accompanying conversion of the  $L_c$  phases of such mixtures to the  $L_\beta$  phase is probably too broad and/or too weak to be resolved by the DSC

protocols used here. However, our analyses of the temperature-dependent changes in the FTIR spectra exhibited by the DMPE:TMCL (10:90) mixture indicates that its  $L_c/L_\beta$  phase transformation is centered near  $13.5\text{ }^\circ\text{C}$  and spans the  $8\text{--}19\text{ }^\circ\text{C}$  temperature range (data not shown).

Illustrated in Fig. 8 are spectra which typify the composition-dependent changes observed in the C=O stretching and  $\text{CH}_2$  scissoring absorption bands of the IR spectra exhibited after prolonged low temperature incubation of the binary mixtures of TMCL:DMPE. The significant features of the data shown are as follows. First, throughout the composition range in which DMPE:TMCL forms  $L_c$  phases (i.e.,  $\geq 10\text{ mol}\%$  TMCL), the infrared spectroscopic signatures of the  $L_c$  phases formed differ markedly from those exhibited by the  $L_c$  phases of DMPE. We thus conclude that the structural characteristics of all of the  $L_c$  phases formed by the DMPE:TMCL mixtures differ from those of the  $L_c$  phases of DMPE. Second, after prolonged incubation at low temperature, the spectroscopic signatures of the mixture containing 95 mol% DMPE are essentially indistinguishable from those exhibited by the  $L_\beta$  phases of all of the DMPE:TMCL mixtures examined. This observation implies that  $L_c$  phase formation is probably unlikely in mixtures containing  $\geq 95\text{ mol}\%$  DMPE, and that the structural characteristics of the  $L_\beta$ -type lamellar gel phases formed by all of the mixtures are probably similar. Third, the spectroscopic signatures of the  $L_c$  phases formed by mixtures containing  $\geq 10\text{ mol}\%$  TMCL show a progressive gradation of properties as the TMCL content of the mixture increases. Throughout the composition range in which  $L_c$  phases are formed, the broad C=O absorption band centered near  $1735\text{ cm}^{-1}$  seems to be a summation of four components centered near  $1742$ ,  $1734$ ,  $1723$  and  $1710\text{ cm}^{-1}$  (Fig. 8). With DMPE-rich mixtures, the dominant features of the C=O stretching band are the components centered near  $1742$  and  $1723\text{ cm}^{-1}$  and, as the TMCL content of the mixtures increases, the areas these two components progressively decrease relative to the areas of the other two components. Also, in the  $\text{CH}_2$  scissoring region, the main absorption near  $1468\text{--}1470\text{ cm}^{-1}$  appears to be a summation of sharp and broad components centered near  $1471\text{ cm}^{-1}$  and  $1468\text{ cm}^{-1}$ , and as the TMCL content of the mixtures increases, the relative intensity of the sharp component near  $1471\text{ cm}^{-1}$  increases progressively relative to area of the broader component near  $1468\text{ cm}^{-1}$  (Fig. 8). It thus appears that the characteristics of the components of the C=O stretching and the  $\text{CH}_2$  scissoring bands, which become progressively

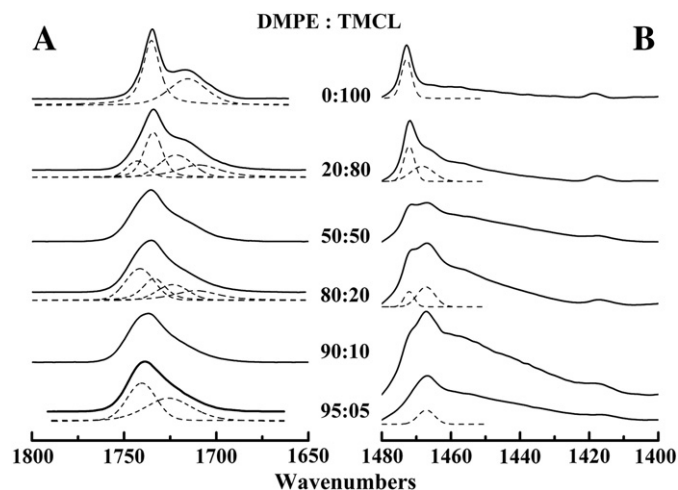


**Fig. 8.** Composition-dependent changes in the contours of C=O stretching (panel A) and  $\text{CH}_2$  scissoring bands (panel B) exhibited by binary mixtures of DMPE and TMCL. The absorbance spectra shown were observed with the binary mixtures indicated and were acquired at  $0\text{ }^\circ\text{C}$  after sample prolonged equilibration at low temperatures. To facilitate comparison, the corresponding spectra exhibited by pure TMCL bilayers are also shown, along with examples of our component analyses of some of the spectra. The latter are shown as dashed lines that were offset to facilitate clarity.

dominant as the TMCL content of the mixtures increases, are quite similar to those exhibited by the pure  $L_c$  phase of pure TMCL, and that those which are dominant in the DMPE-rich mixtures are similar to those observed in the  $L_{\beta}$  phases of all mixtures studied here. In turn, these observations imply that the structural characteristics of the  $L_c$  phases formed by mixtures of TMCL and DMPE are comparable to those of a mixture of a TMCL-like  $L_c$  phase and a  $L_{\beta}$  phase. This possibility was further investigated by spectral subtraction analysis.

The spectra labeled III in Fig. 9 were generated by a weighted subtraction (~65%) of the spectra of the  $L_{\beta}$  phase (spectra II) from those of the  $L_c$  phase (spectra I) formed by an equimolar mixture of DMPE and TMCL, and are virtually indistinguishable from those exhibited by the  $L_c$  phase formed by bilayers of pure TMCL (spectra IV). Also, although spectra comparable in form to those labeled III were typical of those generated in our analyses of the  $L_c$  phases formed by all of the DMPE:TMCL mixtures examined, we generally found that the weighting coefficients required to generate such spectra increased progressively as the TMCL content of the mixtures increased, though not in direct proportion to the increase in the TMCL content (data not shown). However, one should note that the basis of the spectroscopic differences reflected in the spectra generated by the subtraction procedures arises from differences in the relative abundances of the structural constituents of the mixture and not compositional differences *per se*. Nevertheless, these observations strongly support the idea that the structural characteristics of the  $L_c$  phase formed by the TMCL:DMPE mixtures are consistent with those of a mixture composed of a TMCL-like  $L_c$  phase and the  $L_{\beta}$  phase. The implications of this finding as regards the miscibility of DMPE and TMCL are explored in the Discussion below.

#### 4. Discussion

In this study we used a combination of high-sensitivity DSC and FTIR spectroscopy to characterize the thermotropic phase behavior and organization of model bilayers composed of binary mixtures of DMPE and TMCL. The combination of these two techniques enabled a fairly detailed thermodynamic characterization of the polymorphic phases formed and a reasonably accurate mapping of their phase boundaries and structural characteristics. The results are summarized in the temperature-composition pseudo phase diagram shown in Fig. 10, and to our knowledge, this work is the first study of a PE:CL mixture in which all of the fatty acyl chains of the components are identical. The phase boundaries shown therein were estimated from

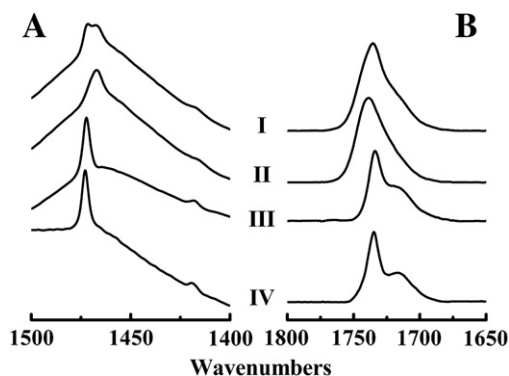


**Fig. 9.** The  $\text{CH}_2$  bending (Panel A) and  $\text{C}=\text{O}$  stretching (Panel B) regions of the infrared spectra exhibited by a binary 50:50 (mol:mol) mixture of DMPE and TMCL. The absorbance spectra shown were generated under the following conditions: I. Low temperature phase ( $0^\circ\text{C}$ ) formed after extensive equilibration at low temperature; II. Low temperature phase ( $0^\circ\text{C}$ ) initially formed upon cooling from high temperature; III. Generated by subtraction of spectra II (~65%) from spectra I; IV. Lamellar crystalline phase ( $0^\circ\text{C}$ ) formed by bilayers of pure TMCL.

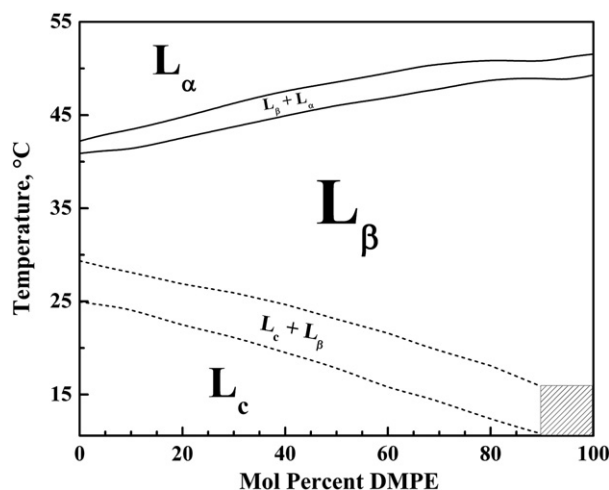


**Fig. 10.** Temperature-composition pseudo phase diagrams of binary mixtures of DMPE and TMCL. The boundaries of the  $L_c/L_{\alpha}$  phase transition of pure DMPE are not included in this diagram. The phase boundaries shown represent the temperature range which encompasses 5% to 95% of the total area under the DSC heating endotherm. Phase assignments were made by FTIR spectroscopic measurements and the phase boundaries of the  $L_c/L_{\beta}$  phase transitions of mixtures containing less than 20 mol % TMCL were estimated by FTIR spectroscopy. The hatched box in the lower right corner of the phase diagram defines an area of uncertainty in the definition of the phase boundaries of the  $L_c/L_{\beta}$  phase transitions of the mixtures.

the area integrals of the DSC thermograms (5–95% total area) and approximate the coexistence ranges of the  $L_{\beta}$  and  $L_{\alpha}$  phases over the entire composition range, and of the coexistence ranges of the  $L_c$  and  $L_{\beta}$  phases exhibited by pure TMCL and by all mixtures in the composition range  $\geq 10$  mol% TMCL. One should note, however, that the phase boundaries shown are, by definition, narrower than those defining the “real” phase-coexistence region and it is highly probable that the narrowing is disproportionately greater with the broader thermograms observed in the midrange of the phase diagram. Also, phase boundaries are not shown for transitions involving the  $L_c$  phases of mixtures containing 0 to  $<10$  mol% TMCL because  $L_c/L_{\beta}$  phase transitions are not defined in the composition range  $>0$  to  $<10$  mol% TMCL, and because the properties of the  $L_c$  phase of pure DMPE are discontinuous from those of the  $L_c$  phases exhibited by all other mixtures studied. Nevertheless, the data show that over the entire composition range, these mixtures exhibit highly energetic and relatively sharp hydrocarbon chain-melting phase transitions, which are all manifest by complex, multi-component DSC thermograms, the contours of which differ upon heating and cooling. Moreover, although the midpoint temperatures of the  $L_{\beta}/L_{\alpha}$  phase transitions of the mixtures all fall within the range bracketed by the hydrocarbon chain-melting phase transition temperatures of TMCL and DMPE, the composition-dependent changes in these  $L_{\beta}/L_{\alpha}$  phase transition temperatures describe a non-linear function in which the observed transition temperatures are higher than those expected of a system in which there is ideal mixing of the two components at or near to the  $L_{\beta}/L_{\alpha}$  phase transition temperatures of the mixtures (see Fig. 3A). Together, these observations clearly indicate that, at the very least, there is non-ideal mixing of the two components throughout the composition range studied. They also suggest that within these mixtures, domain size and structure may vary significantly on either side of the gel/liquid-crystalline phase transition temperature, implying that the miscibility of the two components changes at the transition between the gel and liquid-crystalline phases of these mixtures. Suggestions of non-ideal mixing and overall poor miscibility of cardiolipin with another phospholipid are common themes in most previous studies of mixtures of cardiolipin with other phospholipids [see 28 and references cited therein]. In such studies, the effects of headgroup composition on overall miscibility are often clouded by



uncertainties arising from the known effect of variations in fatty acyl group length and degree of unsaturation on phospholipid miscibility, and by the fact that the differences between the hydrocarbon chain-melting phase transition temperatures of the components are often quite large ( $\geq 30$  °C) [see 28 and references cited therein]. In this study, the fact that poor miscibility is still apparent when the fatty acyl chains of the components are identical and the difference between their  $L_{\beta}/L_{\alpha}$  phase transition temperatures is modest ( $\sim 10$  °C), thus suggests the influence of other factors that are not normally considered in studies of this type. Interestingly, however, the calorimetric data also show that the enthalpy changes associated with the  $L_{\beta}/L_{\alpha}$  phase transitions of these binary mixtures closely follows the curve which describes the changes in the mol fraction of TMCL chains as a function of the composition of the mixture (see Fig. 3B). This observation indicates that regardless of the composition of the mixture, the mean per chain enthalpy associated with the melting of the tetradecanoyl chains of the DMPE and TMCL components of the mixture are essentially the same, consistent with the observation that the per chain normalized enthalpy ( $\sim 3$  kcal/mol) is compatible with those observed at the  $L_{\beta}/L_{\alpha}$  type phase transitions of most of the tetradecanoyl phospho- and glyco-glycerolipids that have been examined so far. This similarity in the per chain melting enthalpy of the DMPE and TMCL components of these mixtures also suggests that the non-ideality, which was inferred from the composition-dependent changes in the  $L_{\beta}/L_{\alpha}$  transition temperatures of the various mixtures examined, is largely entropically driven and is most probably a reflection of composition-dependent changes in preferential interactions between and overall miscibility of the components of the mixtures at temperatures near to  $T_m$ .

We also find that after equilibration at low temperature, DMPE:TMCL mixtures which contain at least 20 mol% TMCL exhibit a lower temperature transition, which arises from the conversion of a  $L_c$  to a  $L_{\beta}$  phase. Although not commonly observed in lipid mixtures, such phenomena have been observed in membranes composed of binary mixtures of DMPC and DMPG [35] and in the multi-component biological membranes isolated from fatty acid-homogeneous *Acholeplasma laidlawii* B [36]. As previously noted with the  $L_c$  phases formed in binary mixtures of DMPC and DMPG, the composition of the mixture is a major determinant of the thermodynamic characteristics of the  $L_c/L_{\beta}$  phase transitions observed. However, unlike the DMPC:DMPG mixtures, the midpoint temperatures and enthalpy values of the  $L_c/L_{\beta}$  transitions exhibited by the DMPE:TMCL mixtures decrease progressively as the DMPE content of the mixture increases, and discrete  $L_c/L_{\beta}$  transitions are not calorimetrically resolved when the DMPE content of the mixture exceeds 80 mol%. It thus appears that the formation of  $L_c$  phases within binary mixtures of DMPE and TMCL is largely driven by the TMCL content of the mixture, and the fact that the transition temperatures and transition enthalpies of the  $L_c/L_{\beta}$  phase transitions also decrease with decreases in the TMCL content of the mixture further suggests that the thermodynamic stabilities of the  $L_c$  phases formed are determined by the TMCL content. This aspect of the behavior of these DMPE:TMCL mixtures also differs markedly from that noted in comparable studies of binary mixtures or DMPC and DMPG, in which the apparent thermodynamic stability of the  $L_c$  phases formed seemed to be dependent on the probability of 1:1 contacts between the two components [35].

Our FTIR spectroscopic studies provided several important clues about the structural characteristics of the polymorphic phases formed by these mixtures, which enabled a fairly accurate assignment of the various phases formed and the construction to the temperature-composition pseudo phase diagram shown in Fig. 10. For example, although  $L_c/L_{\beta}$  phase transitions were not calorimetrically detected in mixtures containing less than 20 mol% TMCL, such structural transformations were detected spectroscopically in mixtures containing as little as 10 mol% TMCL (see Fig. 8). However, the FTIR spectroscopic data also suggest that the formation of  $L_c$  phases is

unlikely when the TMCL content of these mixtures falls significantly below 10 mol%. This observation is particularly interesting when viewed against the fact that pure DMPE bilayers spontaneously form  $L_c$  phases when incubated at low temperatures under conditions comparable to those used here [30]. It thus appears that the presence of small amounts of TMCL in DMPE-rich mixtures inhibits the formation of crystalline structures comparable to those of the  $L_c$  phases formed by pure DMPE. Comparable phenomena were also observed in studies of binary mixtures of DMPC and DMPG, in which case the incorporation of small amounts of DMPC in DMPG-rich mixtures (or DMPG in DMPC-rich mixtures) seems to inhibit the formation of crystalline structures comparable to those formed in membranes composed entirely of the dominant component [35].

The FTIR spectroscopic data also showed that the structural characteristics of the  $L_{\beta}$  phases formed by all DMPE:TMCL mixtures are essentially similar, and that the structural features of the  $L_c$  phases formed by these mixtures are consistent with those expected of mixtures composed of the  $L_{\beta}$  phase and varying amounts of a TMCL-like  $L_c$ -like phase. In principle, these observations can be rationalized by suggesting that the TMCL and DMPE components of the mixtures are poorly miscible in the gel phase, and that they become progressively less miscible upon cooling, such that at temperatures well below  $T_m$ , TMCL tends to phase separate into TMCL-rich domains from which the nucleation and growth of a TMCL-rich  $L_c$  phase eventually occurs. This suggestion is consistent with all of our experimental observations of the  $L_c$  phase and with the inferences drawn from our calorimetric observations of the  $L_{\beta}/L_{\alpha}$  phase transitions of these mixtures (see above). Also, because the structural characteristics of the  $L_c$  phases formed by these mixtures are essentially similar across the composition range (see FTIR spectroscopic data), the observed composition-dependent changes in thermodynamic characteristics of the  $L_c$  phases can be also rationalized on the basis of variations in the mean domain sizes of the  $L_c$  phases formed. An enhancement of the apparent thermodynamic stability of lipid  $L_c$  phases through increases in mean domain size have been inferred in studies of the  $L_c$  phases formed in pure TMCL membranes [31], and in previous studies of the composition-dependent changes in the apparent thermodynamic stabilities of the  $L_c$  phases formed in binary mixtures of DMPC and DMPG [35]. Moreover, since TMCL-like  $L_c$  phases were spectroscopically detected in DMPE-rich mixtures containing as little as 10 mol% TMCL (see Fig. 8), it may well be that DMPE and TMCL are highly immiscible under conditions favorable to the formation of the  $L_c$  phases. In considering the possible reasons why such may be the case, we note that the packing requirements of TMCL, a quadruple-chained amphiphile, will probably differ markedly from those of DMPE, a double-chained amphiphile. It is therefore possible that the poor miscibility of the components of these mixtures may actually be driven by the differences between the packing requirements of the double-chained and quadruple-chained amphiphiles, and not necessarily between the TMCL and DMPE headgroups *per se*. The suggestion that cardiolipin is intrinsically poorly miscible with most common double-chained phospholipids may also be biologically relevant. It is generally observed that CL is a relatively minor component of the cell membranes *in vivo*, and that it tends to be preferentially associated with the membrane proteins, for which CL seems to be required for the maintenance of normal function [12–18]. The poor miscibility of CL with other membrane lipids provides a natural mechanism for facilitating the preferential association of CL with membrane proteins.

Finally, we note that despite the internal consistency of the interpretation presented above, our experimental results do not exclude the possibility of significant DMPE participation in the formation of the  $L_c$  phases formed by these mixtures. As noted above, our spectroscopic characterization the  $L_c$  phases of these mixtures is that of mixtures composed of structural components that are akin to the  $L_{\beta}$  phase and the  $L_c$  phase of TMCL. However, our

experimental data could also be rationalized by suggesting that when mixtures are cooled to temperatures well below the  $T_m$ , the TMCL components of these mixtures serve as nucleation sites for the assembly of structures akin to the  $L_c$  phases formed by pure TMCL. This suggestion can explain all of our data on the  $L_c$  phases formed by these mixtures, including the fact that the inclusion of small amounts of TMCL in DMPE-rich mixtures seems to inhibit the formation of DMPE-like crystalline structures. However, since our structural assignments are based entirely on spectroscopic indicators of packing interactions between hydrocarbon chains and of hydration and hydrogen-bonding interactions in the polar/apolar interfaces of the lipid bilayer, our spectroscopic data are not specific to the TMCL content of the mixture and the possibility that DMPE molecules may assemble into a TMCL-like  $L_c$  phase cannot be excluded. The resolution of this and other issues raised in these studies, and in particular those related to the seemingly poor miscibility of TMCL with DMPE, and possibly with other double-chained phospholipids, is currently the focus of more intensive study.

## References

- [1] D. Marsh, Handbook of Lipid Bilayers, CRC Press, Boca Raton, 1990.
- [2] K. Simons, E. Ikonen, Functional rafts in cell membranes, *Nature* 387 (1997) 569–572.
- [3] L.J. Pike, Lipid rafts: bringing order to chaos, *J. Lipid Res.* 44 (2003) 655–667.
- [4] M. Edidin, The state of lipid rafts: from model membranes to cells, *Annu. Rev. Biophys. Biomol. Struct.* 32 (2003) 257–283.
- [5] S. Munro, Lipid rafts: elusive and illusive? *Cell* 88 (2003) 377–388.
- [6] T.P.W. McMullen, R.N.A.H. Lewis, R.N. McElhaney, Cholesterol–phospholipid interactions, the liquid-ordered phase and lipid rafts in model and biological membranes, *Curr. Opin. Colloid Interface Sci.* 8 (2004) 459–468.
- [7] G. Daum, Lipids mitochondria, *Biochim. Biophys. Acta* 822 (1985) 1–42.
- [8] C. Ratledge, S.G. Wilkinson, Fatty acids, related and derived lipids, in: C. Ratledge, S.G. Wilkinson (Eds.), *Microbial Lipids*, Academic Press, London, 1988, pp. 23–53.
- [9] W.M. O'Leary, S.G. Wilkinson, Gram-positive bacteria, in: C. Ratledge, S.G. Wilkinson (Eds.), *Microbial Lipids*, Academic Press, London, 1988, pp. 117–201.
- [10] S.G. Wilkinson, Gram-negative bacteria, in: C. Ratledge, S.G. Wilkinson (Eds.), *Microbial Lipids*, Academic Press, London, 1988, pp. 299–488.
- [11] F.L. Hoch, Cardiolipins and biomembrane function, *Biochim. Biophys. Acta* 1113 (1992) 71–133.
- [12] Y. Kagawa, A. Kandrach, E. Racker, Partial resolution of the enzymes catalyzing oxidative phosphorylation. XXVI. Specificity phospholipids required energy transfer reactions, *J. Biol. Chem.* 248 (1973) 676–684.
- [13] M.P. Dale, N.C. Robinson, Synthesis of cardiolipin derivatives with protection of the free hydroxyl: its application to the study of cardiolipin stimulation of cytochrome c oxidase, *Biochemistry* 27 (1988) 8270–8275.
- [14] S. Arnold, B. Kadenbach, Cell respiration is controlled by ATP, an allosteric inhibitor of cytochrome c oxidase, *Eur. J. Biochem.* 249 (1997) 350–354.
- [15] C. Lange, J.H. Nett, B.L. Trumpower, C. Hunte, Specific roles of protein–phospholipid interactions in the yeast cytochrome *bc1* complex structure, *EMBO J.* 20 (2001) 6591–6600.
- [16] K.E. McAuley, P.K. Fyfe, J.P. Ridge, N.W. Isaacs, R.J. Cogdell, M.R. Jones, Structural details of an interaction between cardiolipin and an integral membrane protein, *Proc. Natl. Acad. Sci. USA* 96 (1999) 14706–14711.
- [17] R. Serrano, B.J. Banner, E. Racker, Purification and properties of the proton-translocating adenosine triphosphatase complex of bovine heart mitochondria, *J. Biol. Chem.* 251 (1976) 2453–2461.
- [18] F.L. Hoch, Cardiolipins and mitochondrial proton-selective leakage, *J. Bioenerg. Biomembr.* 30 (1998) 511–532.
- [19] K.E. McAuley, P.K. Fyfe, J.P. Ridge, N.W. Isaacs, R.J. Cogdell, M.R. Jones, Structural details of an interaction between cardiolipin and an integral membrane protein, *Proc. Natl. Acad. Sci. U.S.A.* 96 (1999) 14706–14711.
- [20] T. Tanaka, J.F. Strauss, Stimulation of luteal mitochondrial cholesterol side-chain cleavage by cardiolipin, *Endocrinology* 110 (1982) 1592–1598.
- [21] R.C. Tuckey, K.J. Cameron, Catalytic properties of cytochrome P-450(SCC) purified from the human placenta—comparison to bovine cytochrome P-450(SCC), *Biochim. Biophys. Acta* 1163 (1993) 185–194.
- [22] P. Kisselev, R.C. Tuckey, S.T. Woods, T. Triantopoulos, D. Schwartz, Enzymatic properties of vesicle-reconstituted human cytochrome P450SCC (CYP11A1)—differences in functioning of the mitochondrial electron-transfer chain using human and bovine adrenodoxin and activation by cardiolipin, *Eur. J. Biochem.* 260 (1999) 768–773.
- [23] M.C. Wakeham, R.B. Sessions, M.R. Jones, P.K. Fyfe, Is there a conserved interaction between cardiolipin and the Type II bacterial reaction center? *Biophys. J.* 80 (2001) 1395–1405.
- [24] H.U. Koch, R. Haas, W. Fischer, The role of lipoteichoic acid biosynthesis in membrane lipid metabolism of growing *Staphylococcus aureus*, *Eur. J. Biochem.* 138 (1984) 357–363.
- [25] S.A. Short, D.C. White, Metabolism of phosphatidylglycerol, lysylphosphatidylglycerol and cardiolipin of *Staphylococcus aureus*, *J. Bacteriol.* 108 (1971) 219–226.
- [26] Y. Kanemasa, T. Yoshioka, H. Hayashi, Alteration of the phospholipid composition of *Staphylococcus aureus* cultures in medium containing NaCl, *Biochim. Biophys. Acta* 280 (1972) 444–450.
- [27] F.L. Hoch, Cardiolipins and mitochondrial proton-selective leakage, *J. Bioenerg. Biomembr.* 30 (1998) 511–532.
- [28] R.N.A.H. Lewis, R.N. McElhaney, The physicochemical properties of cardiolipin bilayers and cardiolipin-containing lipid membranes, *Biochim. Biophys. Acta* 1788 (2009) 2069–2079.
- [29] H.H. Mantsch, C. Madec, R.N.A.H. Lewis, R.N. McElhaney, Thermotropic phase behavior of model membranes composed of phosphatidylcholines containing isobranched fatty acids. 2. Infrared and  $^{31}\text{P}$ -NMR spectroscopic studies, *Biochemistry* 24 (1985) 2440–2446.
- [30] R.N.A.H. Lewis, R.N. McElhaney, Calorimetric and spectroscopic studies of the polymorphic phase behavior of a homologous series of n-saturated 1, 2-diacyl phosphatidylethanolamines, *Biophys. J.* 64 (1993) 1081–1096.
- [31] R.N.A.H. Lewis, D. Zweytick, G. Pabst, K. Lohner, R.N. McElhaney, Calorimetric, X-ray diffraction, and spectroscopic studies of the thermotropic phase behavior and organization of tetramyristoyl cardiolipin membranes, *Biophys. J.* 92 (2007) 3166–3177.
- [32] Yao, H., I. Hatta, R. Koynova, and B. Tenchol, Time resolved and x-ray diffraction studies at low scan rates II. On the fine structure of the phase transition of dipalmitoyl phosphatidylethanolamine, *Biophys. J.* 61 (1992) 683–693.
- [33] R.N.A.H. Lewis, R.N. McElhaney, Vibrational spectroscopy of lipids, in: J.M. Chalmers, P.R. Griffiths (Eds.), *The Handbook of Vibrational Spectroscopy*, vol. 5, John Wiley & Sons, Ltd, 2002, pp. 3447–3464.
- [34] R.N.A.H. Lewis, R.N. McElhaney, FTIR spectroscopy in the study of hydrated lipids and lipid bilayer membranes, in: H.H. Mantsch, D. Chapman (Eds.), *Infrared Spectroscopy of Biomolecules*, John Wiley & Sons, N. Y, 1996, pp. 159–202.
- [35] R.N.A.H. Lewis, Y.-P. Zhang, R.N. McElhaney, Calorimetric and spectroscopic studies of the phase behavior and organization of lipid bilayer model membranes composed of binary mixtures of dimyristoyl phosphatidylcholine and dimyristoyl phosphatidylglycerol, *Biochim. Biophys. Acta* 168 (2005) 203–214.
- [36] C. Seguin, R.N.A.H. Lewis, H.H. Mantsch, R.N. McElhaney, Calorimetric studies of the thermotropic phase behavior of cells, membranes and lipids from fatty acid homogenous *Acholeplasma laidlawii* B, *Israel J. Med. Sci.* 23 (1987) 403–407.